Applied Thermal Engineering 29 (2009) 1648–1656

Contents lists available at ScienceDirect

Applied Thermal Engineering

journal homepage: www.elsevier.com/locate/apthermeng

Thermal comfort enhancement by using a ceiling fan

Son H. Ho, Luis Rosario, Muhammad M. Rahman *

Department of Mechanical Engineering, University of South Florida, 4202 E. Fowler Avenue, ENB 118, Tampa, FL 33620, USA

ARTICLE INFO

Article history:
Received 19 May 2006
Accepted 15 July 2008
Available online 25 July 2008

Keywords:
Ceiling fan
Thermal comfort
Predicted mean vote
Air conditioning

ABSTRACT

A parametric analysis on the effect of using a ceiling fan in an air-conditioned room is performed by two-dimensional (2D) numerical simulation of steady state airflow and heat transfer. Thermal comfort analysis is done for a person standing in a room with an inlet and an outlet for air conditioning and a ceiling fan. Representative three-dimensional (3D) simulation is also performed for the comparison of results obtained by using 2D and 3D models. Distributions of velocity, temperature, and relative humidity are presented. Different cases in which the ceilings fan may be not in use or in use with different air speed normal to the plane of fan blades due to different rotational speeds are considered. Predicted mean vote is computed and used to assess the thermal comfort characteristics. It is found that as the normal air speed from the fan increases, thermal comfort significantly shifts toward the cooler scale to allow higher supply air temperature or higher heat load in the room while maintaining the same comfort level.

1. Introduction

Thermal comfort depends on many factors, in which, temperature, humidity, and air speed are among the most important ones. In cooling scenarios, although low temperature is the first choice for comfort control, moderate air speed as a breeze can enhance thermal comfort at higher temperature by "wind chill" effect. In residential and commercial buildings, temperature control is achieved by using air conditioners, while air speed can be increased by using ceiling fans. The proper use of a ceiling fan in an air-conditioned space can result in better thermal comfort and energy savings. Rohles et al. [1,2] studied the effectiveness of ceiling fans in enhancing comfort experimentally by examining 256 subjects under various temperature and air velocity in an environment chamber equipped with a ceiling fan. The results showed that an air plume from a ceiling fan with velocity between 0.5 and 1.0 m/s compensates for a 2.8–3.3 °C temperature change; this represents an energy saving of 15–18%. Morton-Gibson et al. [3] investigated the effects of ceiling fans or individual fans on thermal comfort in an office building and found that operating fans for about 1000 h per year at 26.7 °C results in approximately the same comfort levels as 24.4 °C without fans and that the resulting savings are more than the cost and energy usage of the fans. James et al. [4] presented a simulation study using energy balance approach to show the relationship of residential cooling energy use to interior thermostat set points and fan use. This study considered 400 Florida households. It is found that significant cooling energy use savings are possible if ceiling fans are used with higher thermostat set points.

The objective of this study is to use numerical modeling to simulate the two-dimensional (2D) airflow and heat transfer in the room, as well as to estimate the thermal comfort factors, and show the effect of the use of the ceiling fan on those parameters. Several parameters can affect fluid flow and heat transfer in the room such as the location of the supply air diffuser, velocity and temperature of airflow from the supply opening, and heat dissipated by the light set and by the fan motor when the fan is in use. A parametric analysis of one case with air conditioner with no ceiling fan and three other cases with different fan normal air speed are studied. One representative simulation on a three-dimensional (3D) model is also performed to assess the capability of the 2D model. The detailed evaluation of fluid flow, heat transfer, and water vapor diffusion in the entire region will be a very valuable contribution towards the design optimization of air handling systems.

2. Mathematical model

A typical air-conditioned room with a ceiling fan is shown in Fig. 1. It includes inlet (supply) and outlet (return or exhaust) openings for the air conditioning system, a ceiling fan suspended from the ceiling in the middle of the room with a light set attached to it, and a person standing under the fan. To predict the indoor thermal environment, it is necessary to determine air velocity, temperature, and relative humidity in the room. This can be done by solving the coupled equations for the conservation of mass (for moist air as the carrying fluid as well as water vapor diffusing

* Corresponding author. Tel.: +1 813 974 5625; fax: +1 813 974 3539.
E-mail address: rahman@eng.usf.edu (M.M. Rahman).

1359-4311/$ - see front matter © 2008 Elsevier Ltd. All rights reserved.
doi:10.1016/j.applthermaleng.2008.07.015

Nomenclature

c_p	specific heat of air, J/(kg K)
D	diffusivity of water vapor in moist air, m^2/s
f_{cl}	ratio of clothed surface area to nude surface area
$\mathbf{g}$	gravitational acceleration vector, m/s^2
h_c	convective heat transfer coefficient, $W/(m^2 K)$
I_{cl}	thermal resistance of clothing in clo units, clo
k	thermal conductivity of air, W/(m K)
l_c	characteristic length scale of the flow, m
l_m	mixing length, m
l_n	distance from the nearest wall, m
M	metabolic heat generation flux, W/m^2 of naked body area
$\mathbf{n}$	normal vector on boundary
p	pressure, Pa
p_w	partial pressure of water vapor in moist air, Pa
p_{ws}	pressure of saturated water, Pa
PMV	predicted mean vote
PPD	predicted percentage dissatisfied
Pr	Prandtl number
q	heat flux, W/m^2
q_w	mass flux of water vapor, $kg/(m^2 s)$
R_{cl}	thermal resistance of clothing, $m^2 K/W$
RH	relative humidity
Sc	Schmidt number
T	temperature; mean temperature (with subscript), °C
u	velocity component (with subscript), m/s
$\mathbf{u}$	velocity vector, m/s
v	mean air speed relative to the body, m/s
V	air speed, m/s
w	concentration (mass ratio) of water vapor, kg/kg of moist air
W	external work, W/m^2 of naked body area

Greek symbols

β	thermal expansion coefficient, K^{-1}
κ	von Karman constant
μ	viscosity of air, kg/(m s)
ρ	density of air, kg/m^3
Ω	integration domain

Subscripts

a	air, ambient
body	on outer surface of body of person
eff	effective
fan	from fan
i	index
j	index
light	on outer surface of light
motor	on outer surface of fan motor
r	radiant
ref	reference
supply	at supply opening
t	turbulent
x	x-direction
y	y-direction
z	z-direction

within it), momentum, and energy of the airflow. We considered a steady state, incompressible flow of moist air as a multi-component fluid composed by dry air and water vapor. Fluid properties are considered as constants except the varying density for buoyancy term in the momentum equation. The equation for the conservation of mass applied to the air mixture as a whole or carrying fluid can be written as

$$\nabla \cdot \mathbf{u} = 0 \tag{1}$$

The buoyancy force term arising from density variation is included by means of the Boussinesq approximation based on the assumptions that variation in fluid density affects only the buoyancy term and fluid density is a function of temperature and species concentration only. For most HVAC applications, the species concentrations are very small such that the dependency of buoyancy term on them can be neglected. The equation for the conservation of linear momentum can be written as

$$\rho \mathbf{u} \cdot \nabla \mathbf{u} = -\nabla p + \mu_{eff} \nabla^2 \mathbf{u} + \rho \mathbf{g} \beta (T - T_{ref}) \tag{2}$$

Assuming that there is no heat generation, thermal conductivity is scalar, energy flux due to inter-diffusion and Dufour effect are negligible, the equation for the conservation of energy is given by

$$\rho c_p \mathbf{u} \cdot \nabla T = k_{eff} \nabla^2 T \tag{3}$$

Assuming that the mass diffusivities of species in air are scalars, thermal diffusion (Soret effect) is negligible, and there is neither source nor chemical reaction, the equation for the conservation of mass of water vapor as carried species can be written as

$$\mathbf{u} \cdot \nabla w = D_{eff} \nabla^2 w \tag{4}$$

For modeling the turbulent flow, the effective viscosity is defined as the sum of the dynamic viscosity of the fluid and eddy viscosity; the latter is estimated by using the mixing length model. Similarly, the effective thermal conductivity is defined as the sum of the physical thermal conductivity of the fluid and a turbulent thermal conductivity, whereas the effective diffusivity of water vapor species is defined as the sum of the physical diffusivity of water vapor in moist air and a turbulent mass diffusivity. The mixing length turbulence model can be represented as

$$\mu_{eff} = \mu + \mu_t \tag{5}$$

$$\mu_t = \rho l_m^2 \sqrt{\left(\frac{\partial u_i}{\partial x_j} + \frac{\partial u_j}{\partial x_i}\right) \frac{\partial u_i}{\partial x_j}} \tag{6}$$

$$l_m = \min\{\kappa l_n, 0.09 l_c\} \tag{7}$$

$$k_{eff} = k + k_t \tag{8}$$

$$k_t = \frac{c_p \mu_t}{Pr_t} \tag{9}$$

$$D_{eff} = D + D_t \tag{10}$$

$$D_t = \frac{\mu_t}{\rho Sc_t} \tag{11}$$

In Eq. (7), κ is the von Karman constant, which usually takes the value of about 0.41 [5]. In Eqs. (9) and (11), Pr_t and Sc_t are the turbulent Prandtl number and the turbulent Schmidt number, respectively, and typically near unity [5]. They were both assigned the value of 0.9 for the computation.

To define the problem completely, appropriate boundary conditions are required on all boundaries of the computational domain. The boundary conditions for velocity are

$$\text{On supply opening}: u_x = V_{supply}, \quad u_y = 0, \quad u_z = 0 \tag{12}$$

$$\text{On fan blade plane}: u_x = 0, \quad u_y = 0, \quad u_z = -V_{fan} \tag{13}$$

$$\text{On all solid surfaces}: u_x = u_y = u_z = 0 \tag{14}$$

$$\text{On symmetry plane}: u_y = 0 \tag{15}$$

The boundary conditions for temperature are

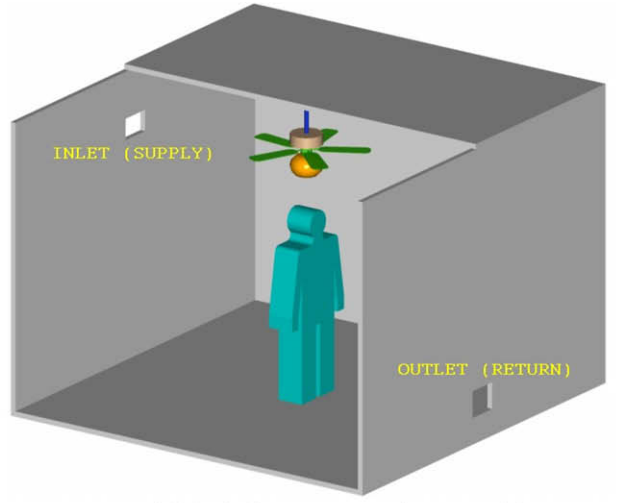

(a) Typical arrangement (not to scale)

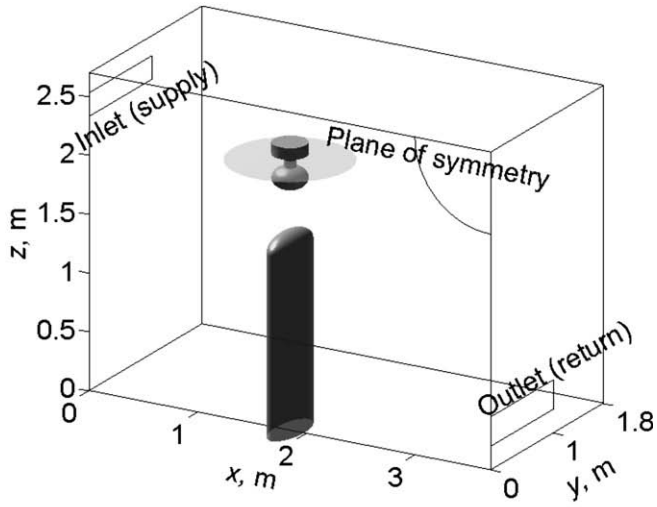

(b) Three-dimensional model (half of the room)

Fig. 1. Room with air conditioner and ceiling fan.

$$\text{On supply opening}: T = T_{\text{supply}} \tag{16}$$

$$\text{On person surface}: T = T_{\text{body}} \tag{17}$$

$$\text{On motor outer surface}: \mathbf{n}\cdot(k_{\text{eff}}\ \nabla T) = q_{\text{motor}} \tag{18}$$

$$\text{On light set surface}: \mathbf{n}\cdot(k_{\text{eff}}\ \nabla T) = q_{\text{light}} \tag{19}$$

$$\text{On other boundary surfaces}: \mathbf{n}\cdot(k_{\text{eff}}\ \nabla T) = 0 \tag{20}$$

The boundary conditions for water vapor concentration are

$$\text{On supply opening}: w = w_{\text{supply}} \tag{21}$$

$$\text{On person surface}: \mathbf{n}\cdot(\rho D_{\text{eff}}\nabla w) = q_{\text{w,body}} \tag{22}$$

$$\text{On other boundary surfaces}: \mathbf{n}\cdot(\rho D_{\text{eff}}\nabla w) = 0 \tag{23}$$

Eqs. (12)–(15) are written for the general case of a 3D model. For 2D models, the component u_y is not present. Eqs. (13) and (18) are only present for the cases where the ceiling fan is in use.

The solution obtained by solving Eqs. (1)–(23) gives the distributions of five (six for 3D model) primary variables: two (three for 3D model) velocity components, pressure, temperature, and water vapor concentration. Based on these, relative humidity can be computed by using the procedure recommended by ASHRAE [6] summarized as

$$\text{RH} = \frac{p_{\text{w}}}{p_{\text{ws}}} \tag{24}$$

where

$$p_{\text{w}} = \frac{(101325 + p)w}{0.62198 + 0.37802w} \tag{25}$$

$$\begin{aligned} p_{\text{ws}} = \exp[&-0.58002206\times10^{4}(T+273.15)^{-1} \\ &+0.13914993\times10^{1}-0.48640239\times10^{-1}(T+273.15) \\ &+0.41764768\times10^{-4}(T+273.15)^{2} \\ &-0.14452093\times10^{-7}(T+273.15)^{3} \\ &+0.65459673\times10^{1}\ln(T+273.15)] \end{aligned} \tag{26}$$

One of the most frequently cited thermal comfort models is the Fanger's model based on steady-state energy balance. This model was originally developed to predict human thermal comfort in office-like environments and has gained wide usage in the HVAC industry because of its simplicity [7]. Predicted mean vote (PMV) is a parameter for assessing thermal comfort in an occupied zone based on the conditions of metabolic rate, clothing, air speed besides temperature and humidity. From the results of the work of Fanger [8] summarized in ASHRAE Handbook [6], the value of PMV is given by

$$\begin{aligned} \text{PMV} = [&0.303\exp(-0.036M)+0.028]\times\{(M-W) \\ &-3.96\times10^{-8}f_{\text{cl}}[(T_{\text{cl}}+273.15)^{4}-(T_{\text{r}}+273.15)^{4}] \\ &-f_{\text{cl}}h_{\text{c}}(T_{\text{cl}}-T_{\text{a}})-3.05[5.733-0.007(M-W) \\ &-0.001p_{\text{w}}]-0.42[(M-W)-58.15]-0.0173M(5.867 \\ &-0.001p_{\text{w}})-0.0014M(34-T_{\text{a}})\} \end{aligned} \tag{27}$$

where

$$\begin{aligned} T_{\text{cl}} = {}&35.7-0.0275(M-W) \\ &-R_{\text{cl}}\{3.96\times10^{-8}f_{\text{cl}}[(T_{\text{cl}}+273.15)^{4}-(T_{\text{r}}+273.15)^{4}] \\ &+f_{\text{cl}}h_{\text{c}}(T_{\text{cl}}-T_{\text{a}})\} \end{aligned} \tag{28}$$

$$h_{\text{c}} = \begin{cases} 2.38(T_{\text{cl}}-T_{\text{a}})^{0.25} & 2.38(T_{\text{cl}}-T_{\text{a}})^{0.25} > 12.1v^{0.5} \\ 12.1v^{0.5} & 2.38(T_{\text{cl}}-T_{\text{a}})^{0.25} \leqslant 12.1v^{0.5} \end{cases} \tag{29}$$

$$f_{\text{cl}} = \begin{cases} 1.0+0.2I_{\text{cl}} & I_{\text{cl}} \leqslant 0.5\text{clo} \\ 1.05+0.1I_{\text{cl}} & I_{\text{cl}} > 0.5\text{clo} \end{cases} \tag{30}$$

$$R_{\text{cl}} = 0.155I_{\text{cl}} \tag{31}$$

PMV values refer to the ASHRAE thermal sensation scale [6] that ranges from −3 to 3 as follows: 3 = hot, 2 = warm, 1 = slightly warm, 0 = neutral, −1 = slightly cool, −2 = cool, −3 = cold.

Predicted percentage dissatisfied (PPD) is used to estimate the thermal comfort satisfaction of the occupant. It is considered that satisfying 80% of occupant is good; that is, PPD less than 20% is good. From [6], the value of PPD can be calculated from a known PMV value as

$$\text{PPD} = 100 - 95\exp(-0.03353\text{PMV}^{4} - 0.2179\text{PMV}^{2}) \tag{32}$$

3. Numerical simulation

The 2D model of the room is shown in Fig. 2. The essential dimensions are denoted in general forms as L1 to L12. The numerical values used for the computations in this paper are assigned as follows: $L1$ = 3.7 m, $L2$ = 2.7 m, $L3$ = 1.85 m, $L4$ = 0.26 m, $L5$ = 1.70 m, $L6$ = 0.10 m, $L7$ = 1.07 m, $L8$ = 2.30 m, $L9$ = 2.33 m, $L10$ = 0.20 m, $L11$ = 0.20 m, and $L12$ = 0.25 m. The crossed regions that represent the person and the light-fan motor assembly are not part of the computational domain. The outer region around the person (enclosed by dashed lines) with the width of L6 is a

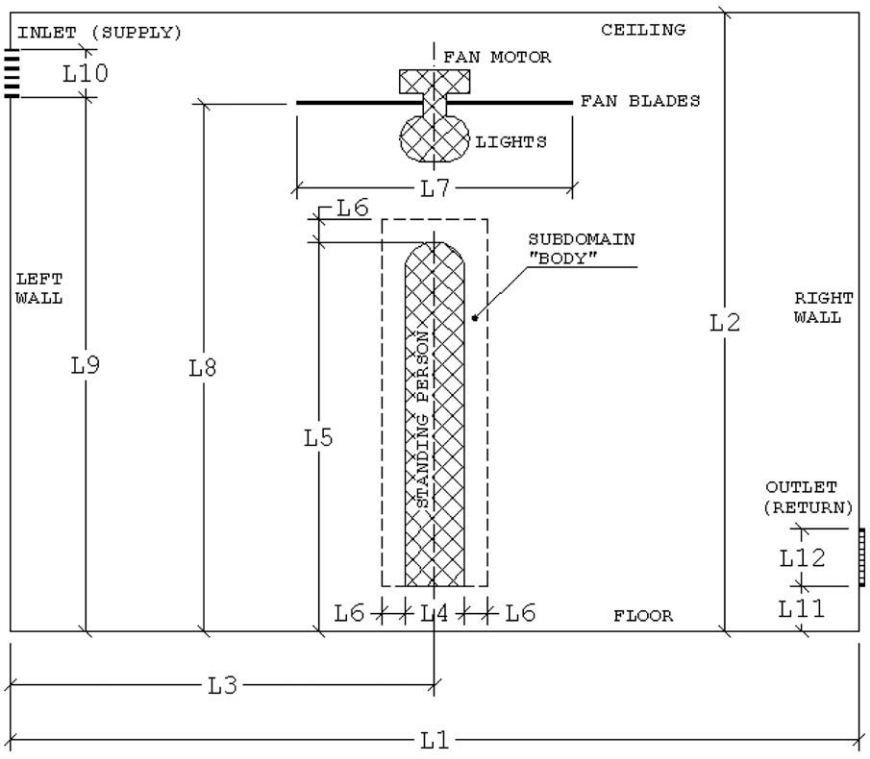

Fig. 2. Two-dimensional model of air-conditioned room with ceiling fan.

computational subdomain named "Body" used for assessing the thermal comfort factors in the surrounding air wrapping around the person to give better evaluation of the comfort level of the person.

The constant fluid properties of air are taken at a reference temperature of $T_{ref} = 22\ ^\circ C = 293\ K$ as follows: $\rho = 1.1967\ kg/m^3$, $\mu = 1.8273 \times 10^{-5}\ kg/(m\ s)$, $c_p = 1.0043\ kJ/(kg\ K)$, $k = 0.025776\ W/(m\ K)$, $\beta = 0.003932\ K^{-1}$, and $D = 2.5449 \times 10^{-5}\ m^2/s$.

The data of imposed air speeds and heat and mass fluxes are taken equivalent values calculated such that the approximation takes into account the effects of finite dimensions of the solid surfaces (the person, fan, light, etc.) in the room. The supply air has a velocity normal to the opening with a speed of $V_{supply} = 1$ m/s. Its temperature and water vapor concentration are $T_{supply} = 22\ ^\circ C$ and $w_{supply} = 0.0148$ kg/kg air. The fan motor gives off a heat flux of $q_{motor} = 10\ W/m^2$ uniformly distributed on its cover if the fan is in use. The light set under the fan gives off a heat flux of $q_{light} = 300\ W/m^2$. The outer surface of the person is considered of constant temperature $T_{body} = 34\ ^\circ C$ and also giving off a mass flux of water vapor due to respiration and sweating of $q_{w,body} = 5 \times 10^{-7}\ kg/(m^2\ s)$. The forced flow from the ceiling fan is characterized by the air velocity V_{fan} normal to the plane of the fan blades. It takes the values of 1.1, 1.3, and 1.5 m/s corresponding to three simulation cases with the fan in use as shown in Table 1.

Eqs. (1)–(23) were solved by using the finite element method. In each element, two (three for 3D model) velocity components, pressure, temperature, and concentration of water vapor were approximated by using the Galerkin procedure [9], which led to a set of algebraic equations that approximately defined the continuum. The distribution of the element size in the computational domain was determined from a series of tests with different numbers of elements in all coordinate directions and for different mesh density around inlet, outlet and objects where high rates of momentum, heat and mass transfer exist. By systematically increasing the number of elements as well as the grading ratios and monitoring the residual distribution for all variables in the computational domain, the mesh needed for accurate computation was determined. For 2D model, a mesh of approximately 37,300 four-node quadrilateral elements was used. For 3D model, a mesh of about 32,600 eight-node hexahedral elements was used.

Table 1
Simulation cases and results of mean air speed in room and around person

2D simulation case #	1	2	3	4
Fan normal air speed V_{fan}, m/s	0	1.1	1.3	1.5
Room mean air speed, m/s	0.235	0.571	0.652	0.743
"Body" mean air speed, m/s	0.223	0.459	0.567	0.63

For 2D model, the fully coupled successive substitution algorithm was used to solve the system of nonlinear algebraic equations. Two convergence criteria were used: relative errors of the solutions and residual of the nonlinear equations. The relative error criterion is considered reached when the relative error of the solution at an iteration compared to that at the previous one is less than a tolerance. On the other hand, the residual criterion checks whether the ratio of the residual vector at an iteration to a reference residual vector, is less than another tolerance. The iterative procedure for the solution is considered converged when both criteria are satisfied. The tolerances of 0.0001 and 0.01 were used for these criteria, respectively. For 3D model, the segregated algorithm was employed and the relative error convergence criterion was used with a corresponding tolerance of 0.001.

After the primary variable fields (velocity, pressure, temperature, and water vapor concentration) were found, relative humidity distribution was computed by using Eqs. (24)–(26). PMV value was calculated for a standing, relaxed person (with metabolic rate of 1.2 met) dressed in summer attire (with clothing insulation of 0.5 clo) using Eqs. (27)–(31). Then PPD was calculated using Eq. (32). The mean temperature and mean air speed can be found by integration as

$$\overline{T} = \frac{\int_{(\Omega)} T \mathrm{d}x\,\mathrm{d}y\,\mathrm{d}z}{\int_{(\Omega)} \mathrm{d}x\,\mathrm{d}y\,\mathrm{d}z} \tag{33}$$

$$\bar{u} = \frac{\int_{(\Omega)} \sqrt{u_x^2 + u_y^2 + u_z^2}\,\mathrm{d}x\,\mathrm{d}y\,\mathrm{d}z}{\int_{(\Omega)} \mathrm{d}x\,\mathrm{d}y\,\mathrm{d}z} \tag{34}$$

where the over-bar represents the mean or average value, and Ω is the domain of interest. In this study, the entire computational domain or the subdomain "Body" around the person are considered for Ω. For 2D models, only two relevant coordinates x and z appear in Eqs. (33) and (34).

4. Results and discussion

Fig. 3 presents the distribution of air velocity, temperature, and relative humidity for the base case, simulation 1, where the ceiling fan is not in use. In Fig. 3a, the velocity field is represented by the streamlines on the filled background with the color proportional to air speed. The cool airflow enters the room through the supply diffuser on the left wall at uniform full speed (1.0 m/s). The incoming flow goes straight horizontally at first since the temperature in the region far from the lights and the person has moderate low temperature that the buoyancy effect is insignificant. As the airflow approaches the middle part of the room where higher temperature distributed around the lights and the person is present, the buoyancy effect becomes stronger and tends to pull the main stream of the airflow down. However, since the inlet airflow has a quite high speed, a small part of the airflow splits up and continues to sweep along the ceiling with reducing speed before it goes down along the right wall to the outlet. The main stream goes down at the lights to the top of the person, sweeps through the upper part of him or her at a relatively high speed. Then the main stream splits again; the main part, still has momentum, bends to the left, slightly touches the floor and goes up, makes a clear strong circulation in the supply side of the room, the other part of the stream moves along the floor to the outlet at reducing speed.

Fig. 3b shows the distribution of temperature for simulation 1. The circulation in the supply side of the room creates a good mixing zone where the temperature is just about the inlet temperature or one, one and a half centigrade degree more. In the exhaust side of the room, since most of the streams with significant momentum just sweep along the ceiling, the wall, or the floor, the air in the major region is moving very slowly. In this region, the heat transfer is mostly occurring by diffusion. In Fig. 3b, the core has a higher temperature and it reduces towards the ceiling, the wall, and the floor, which shows a diffusion pattern. It can be also observed that there are thin layers of high gradient and high temperature around the person and the lights, as well expected.

Fig. 3c is the plot of the distribution of relative humidity, one of the important factors for assessing thermal comfort. Relative humidity is a function of absolute pressure, water vapor concentration, and temperature. Its distribution is computed from Eqs. (24)–(26). Since the gage pressure in the room is found very small, on the order of 1 Pa, compared to the atmospheric pressure, on the order of 101 kPa, it has little effect on relative humidity. The water vapor concentration has some effect on relative humidity, but it is still small compared to the effect of temperature. The higher the temperature is, the lower the relative humidity gets, and vice versa. This explains the identical pattern between the distributions of temperature and relative humidity, except in the opposite direction. Near the lights and the person, since the temperature is quite high, the relative humidity is low. The high relative humidity is concentrated in the supply side of the room where there is low temperature as the result of the strong circulation as discussed previously. On the other hand, the exhaust side of the room has lower relative humidity as the temperature in this region is higher.

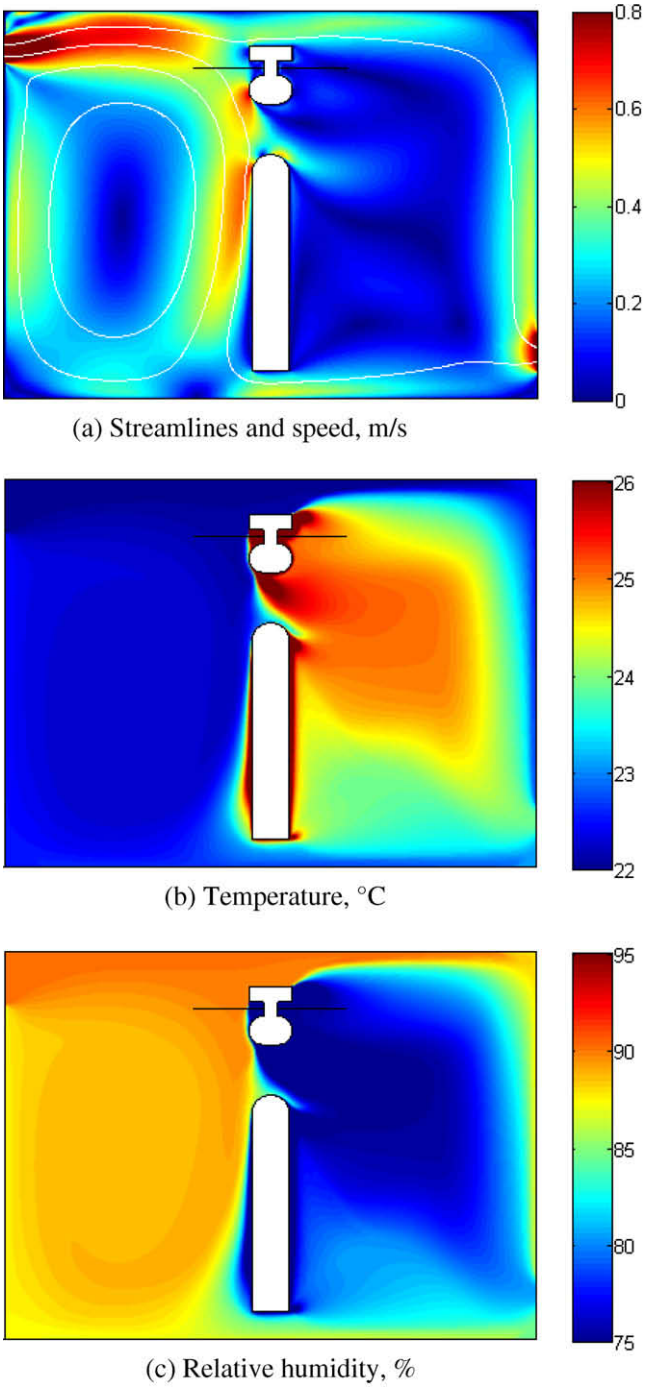

Fig. 3. Distributions of velocity, temperature, and relative humidity for simulation 1.

Fig. 4 presents the distribution of air velocity, temperature, and relative humidity for simulation 2 in which the ceiling fan is in use and it produces a normal (to blades plane) air speed of 1.1 m/s on the same order as the airflow through the supply inlet (1.0 m/s). Fig. 4a shows the airflow field by streamline contours plotted on color-coded speed background. With the presence of the velocity from the ceiling fan, the flow pattern is totally changed. The supply airflow is pulled towards the fan right after entering the room and creates a circulation similar to that in simulation 1, but much stronger. The supply side of the room becomes very well mixed.

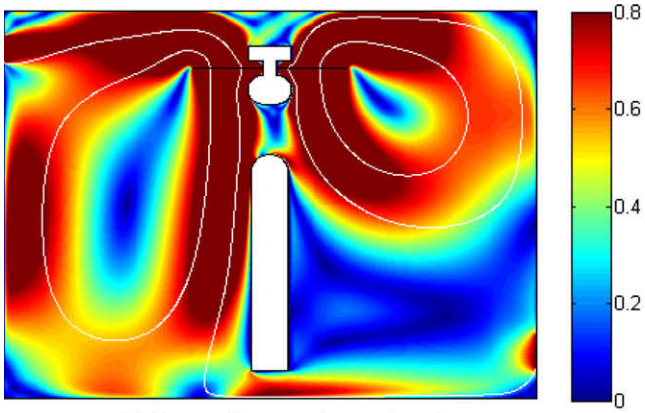

(a) Streamlines and speed, m/s

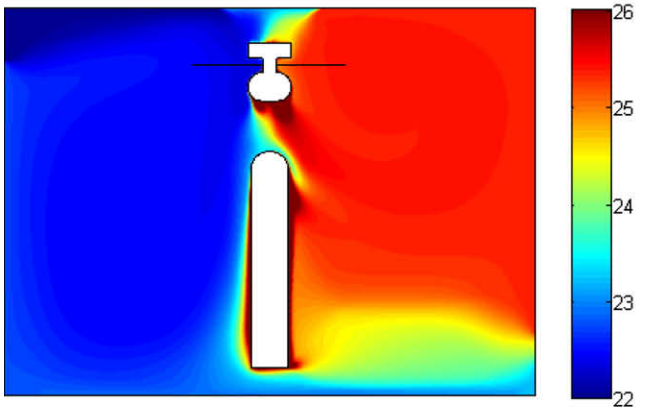

(b) Temperature, °C

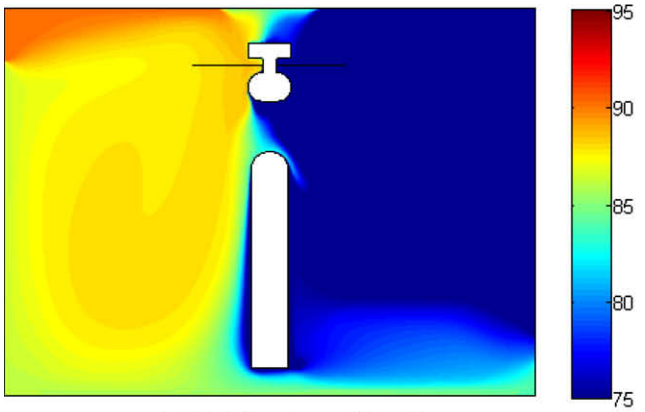

(c) Relative humidity, %

Fig. 4. Distributions of velocity, temperature, and relative humidity for simulation 2.

However, different from simulation 1, the air velocity from the fan also creates a strong circulation in the exhaust side of the room. However, there is no cool air supply on this side to induce the buoyancy effect, thus the circulation created by forced convection is just circling at high region without touching the floor as the circulation in the supply side does. There is also a weak stream sweeping along the floor to the outlet, similar to the base case (simulation 1).

Fig. 4b presents the distribution of temperature for simulation 2. The well-mixed region in the supply side still has lower temperature as in simulation 1. However, the air in the exhaust side of the room is also well mixed, but resulted in more uniformly distributed higher temperature compared to simulation 1 since now the major means of heat transfer is convection. Only a small zone close to the floor still has the diffusion characteristics.

Fig. 4c shows the distribution of relative humidity for simulation 2. This plot, again, shows how strongly the relative humidity depends on temperature in the room. The region in the exhaust side now has lower and uniform relative humidity, since the temperature is higher and uniform. The air in the supply side has higher relative humidity, since the temperature is lower. However, the relative humidity in this region is not as high as that in simulation 1, which suggests that the temperature in this zone is not as low as that in simulation 1. Therefore, it seems that the use of an additional ceiling fan increases the temperature in both sides of the room.

Fig. 5 presents the distributions of air velocity, temperature, and relative humidity for simulation 2 with a 3D model. Fig. 5a shows the 3D streamlines of the airflow starting at nine representative starting points on the area of the supply opening. These streamlines are numbered 1–9 with color-coded legend for easily tracing their paths. In Fig. 5b, the air speed distribution is displayed as respective interpolated filled color on orthogonal slice planes selected in such a way that can reveal the structure of the volumetric data, include planes through the center of the openings and obstacles. Parts (a) and (b) of Fig. 5 can be examined simultaneously to view the image of the flow field in the domain. It can be observed in Fig. 5a that the airflow is pulled through the plane of the fan blades similar to the phenomenon simulated on 2D model in Fig. 4a. The air speed distribution from the 2D model as shown in Fig. 4b resembles that on the plane of symmetry from the 3D model in Fig. 5b. The temperature distribution in the 3D model is shown in Fig. 5c. It can be observed a difference of about or less than 1 °C between the major parts of the two halves of the room, which is also predicted by the 2D model in Fig. 4c except for higher temperature difference (3–4 °C). The mean temperature is found of 1 °C lower than that from the 2D model. Fig. 5d presents the distribution of relative humidity that shows the same pattern but in opposite direction to temperature for the same reason as explained for the 2D cases. These observations suggest that although the 2D model may not describe some details of the complex phenomena of fluid flow and heat transfer in the 3D space of the room, it can predict some important patterns of the phenomena and can approximate quite well the transport phenomena at the symmetry plane. It can be expected that the simulation results from the 3D and 2D models would be different with the 2D model giving higher temperature level and uniformity. Therefore, in cooling scenarios, 2D model is likely to produce conservative assessments in thermal comfort aspects.

Fig. 6 presents the dependence of the mean temperature taken in the entire room as well as in the subdomain "Body" as a thin layer around the person. The values of mean temperature were computed by means of numerical integration based on Eq. (33). In Fig. 6, it can be observed clearly that the temperature does increase as the result of the use of an additional ceiling fan in an air-conditioned room in both the entire domain and the subdomain "Body." More than that, as the air speed from the fan increases, the mean temperature increases as well. This happens because the running of a ceiling fan, while increasing circulation, brings down the still warm air under the ceiling and around the fan motor and keeps circling inside the room without being effectively removed through the outlet and therefore reduces the cooling effect of the increased air speed. This observation, at first, raises a question about what is the point of using a ceiling fan if it makes people hotter instead of cooler.

It is known that thermal comfort is dependent on temperature, relative humidity, and air speed ("chilling effect"). The thermal comfort factor should take into account the effect of the air speed

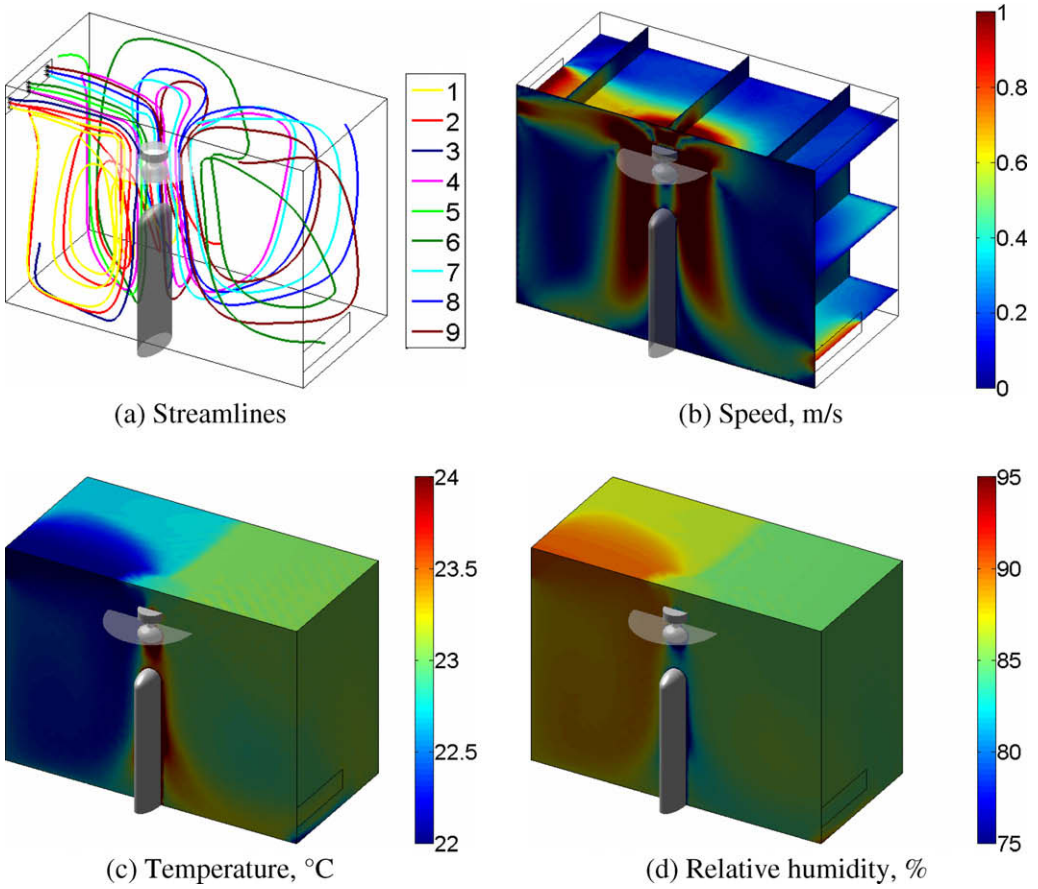

Fig. 5. Distributions of velocity, temperature, and relative humidity for 3D model.

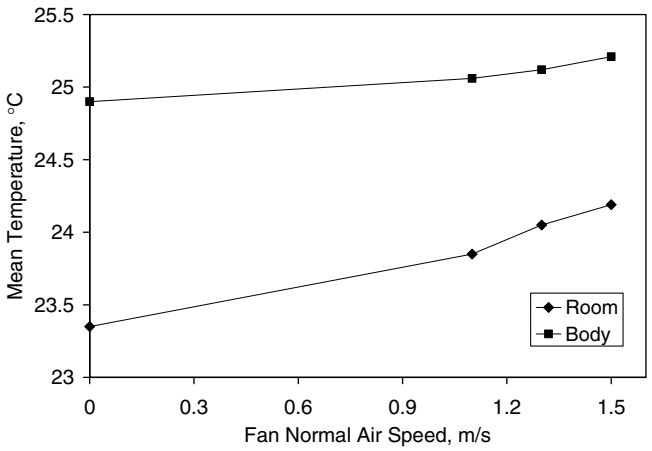

Fig. 6. Effect of fan normal air speed on mean temperature.

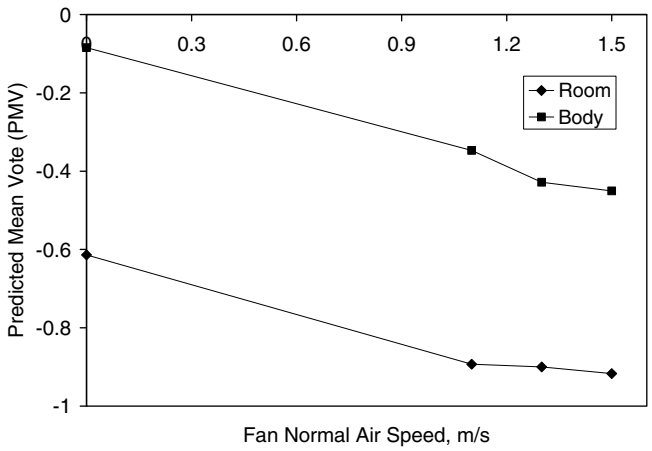

Fig. 7. Effect of fan normal air speed on predicted mean vote (PMV).

around the person. The increases of mean air speed, especially in the subdomain around the person will have significant impact on thermal comfort level. Therefore, the proper factor for the evaluation of thermal comfort for this situation is the PMV as shown in Fig. 7. It can be observed that the PMV for the entire domain is always lower than the PMV calculated for just the subdomain "Body". This implies that in a possible experiment if the measurements were not done close enough to the body the real PMV is always underestimated. As the air speed from the fan increases, the PMV value decreases for both the entire domain and the subdomain "Body". This decreasing trend is very good for the cooling situation. In the case there are additional heat loads, the thermal sensation curves will be shifted up, a decreasing trend is critical to keep the environment inside the comfort zone (from −1 to 1 on the ASHRAE scale). In case there is no additional heat load, the temperature setting for the air conditioner can be raised several degrees for energy savings while maintaining the same comfort level.

For a more detailed evaluation of how the air speed from the ceiling fan affects the local PMV values distributed around the person, Fig. 8 shows a comparison of PMV distribution in the occupied site for simulation 1 (no ceiling fan used) and 2 (with ceiling fan

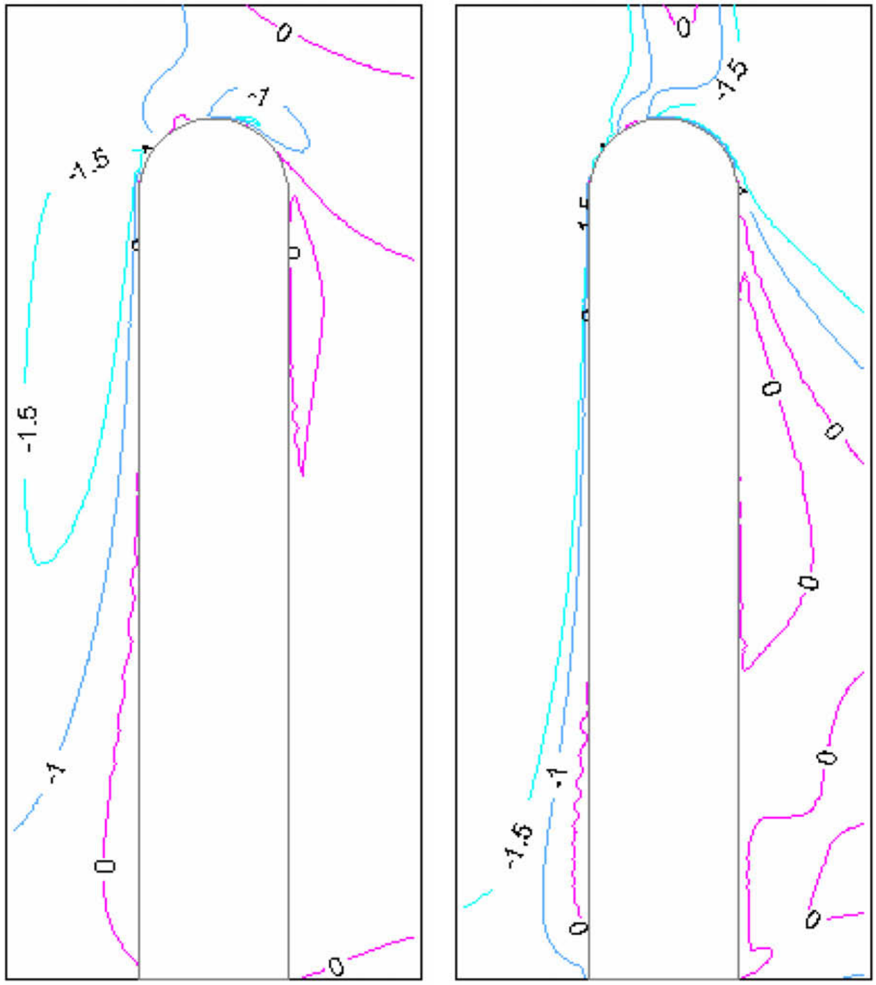

Fig. 8. Comparison of PMV distribution between simulations 1 and 2.

used). For simulation 1, thermal comfort is at most satisfied (PMV = 0) over a large region on the right of the person while it tends to be cooler on the left, especially on the upper part of the body. For simulation 2, under the influence of the ceiling fan, the high PMV regions narrow down on both sides. The low PMV distribution implies that with the use of a ceiling fan, supply air temperature (and thus room temperature) can be increased but thermal comfort level is as satisfied as that for the case of no ceiling fan used.

Table 1 shows the simulation cases and the corresponding results of mean air speed. For each simulation case, two values of mean air speed were computed by means of numerical integration based on Eq. (34), one was taken over the entire domain of the room and the other was taken over the subdomain ‘‘Body" around the person. It can be observed in Table 1 that both mean air speeds increase as the normal air speed from the fan increases and the mean air speed values taken over the entire room are always higher than that taken over the subdomain "Body." The effect of the use of elevated air speed used to increase maximum temperature while maintaining thermal comfort for affected occupants is presented in ASHRAE Standard 55-2204 [10] (Section 5.2.3, Fig. 5.2.3). The data given in this standard applies to a lightly clothed person (with clothing insulation between 0.5 clo and 0.7 clo) who is engaged in near sedentary physical activity (with metabolic rates between 1.0 met and 1.3 met). Those ranges well cover the cases under investigation (0.5 clo, 1.2 met). Using the mean air speeds around the body to estimate the potential increased temperature, the standard shows that for simulation 1, where the air speed is around 0.2 m/s, the offset temperature is almost negligible. On the other hand, for simulations 2–4, where the air speed ranges in about 0.4–0.6 m/s, the offset temperature can reach up to 3–4 °C. These quantitative results confirm the predictions made above based on the average value of PMV (Fig. 7) and PMV distribution contours (Fig. 8) in the occupied zone.

Table 2 compares the ranges of temperature and relative humidity results from the simulations to the typical values at satisfactory thermal comfort given by James et al. [4]. It can be observed that the simulation results are in the similar range as the experimental measurements of thermal comfort.

Table 2
Comparison of temperature, relative humidity, and PPD for thermal comfort

	Temperature (°C)	Relative humidity (%)	PPD (%)
Simulations 1–4	23.4–25.2	75–84	5–23
James et al. [4]	25.5–28.0	60–80	10

5. Conclusions

The results from the numerical simulations provide an insightful understanding of the fluid flow and heat transfer in a room with air conditioner and ceiling fan. For the base case where the fan is not in use, strong air circulations in the inlet side of the room keeps this side cooler due to convective heat transfer, while rather still air in the outlet side have the temperature distribution pattern of diffusive heat transfer. When the fan is used, strong circulations forced by the fan induces convective heat transfer that creates more uniform temperature distribution in both sides of the room. However, these circulations also reduce the total heat removal performance of the system by circulating the heat around the room instead of moving it to the outlet resulting in a slight rise of overall temperature. As the air speed provided by the fan increases, the PMV value decreases toward cooler side and thus over-compensates the temperature rise to leave more adjusting margin for a cooling situation, allowing higher heat load while maintaining the same level of comfort compared to that of the case where there is air conditioner only with no ceiling fan. This characteristic has good impact on energy savings by increasing the temperature setting of the air conditioning system.

References

[1] F.H. Rohles, S.A. Konz, B.W. Jones, Ceiling fans as extenders of the summer comfort envelope, ASHRAE Transactions 89 (1A) (1983) 245–263.
[2] F.H. Rohles, S.A. Konz, B.W. Jones, Enhancing thermal comfort with ceiling fans, Proceedings of the Human Factors Society 26th Annual Meeting (1982) 118–122.
[3] M. Morton-Gibson, P.J. Coutier, W.J. Place, Effects of fan velocity on thermal comfort in an office building, Proceedings of the 10th National Passive Solar Conference, the Solar Energy & Utilities Conference, the Daylighting Applications Conference, the Building with the Sun Conference (1985) 406–409.
[4] P.W. James, J.K. Sonne, R.K. Vieira, D.S. Parker, M.T. Anello, Are energy savings due to ceiling fans just hot air? ACEEE Summer Study on Energy Efficiency in Buildings (1996). FSEC-PF-306-96.
[5] W.M. Kays, M.E. Crawford, B. Weigand, Convective Heat and Mass Transfer, fourth ed., McGraw Hill, New York, 2005.
[6] ASHRAE Handbook – Fundamentals, American Society of Heating, Refrigerating and Air-Conditioning Engineers, Inc., Atlanta, 2005.
[7] Y. Guan, M. Hosni, B.W. Jones, T.P. Gielda, Literature review of the advances in thermal comfort modeling, ASHRAE Transactions 109 (2) (2003) 908–916.
[8] P.O. Fanger, Thermal Comfort Analysis and Applications in Environmental Engineering, McGraw-Hill, New York, 1970.
[9] C.A.J. Fletcher, Computational Galerkin Methods, Springer-Verlag, New York, 1984.
[10] ASHRAE Standard 55-2004 – Thermal Environmental Conditions for Human Occupancy, American Society of Heating, Refrigerating and Air-Conditioning Engineers, Inc., Atlanta, 2004.